ELSEVIER

Journal of Organometallic Chemistry 483 (1994) 39-45

Journal of Organometallic Chemistry

Synthesis and X-ray crystal structure of nitrogen base adducts of decamethylsamarocene: $(C_5Me_5)_2Sm(NH_2CMe_3)$ and $(C_5Me_5)_2Sm(N\text{-}MeIm)_2$

William J. Evans *, Gerd W. Rabe, Joseph W. Ziller

Department of Chemistry, University of California, Irvine, CA, 92717, USA

Received 6 December 1993; in revised form 28 March 1994

Abstract

$(C_5Me_5)_2Sm(THF)_2$ and $(C_5Me_5)_2Sm(THF)$ do not react with Me_3CNH_2 in THF, toluene or hexanes, but $(C_5Me_5)_2Sm$ reacts in toluene to form hexane soluble $(C_5Me_5)_2Sm(NH_2CMe_3)$ (**1**) in high yield. Compound **1** crystallizes from benzene with benzene in the lattice as $(C_5Me_5)_2Sm(NH_2CMe_3)\cdot(C_6H_6)_{0.5}$ in the monoclinic space group $P2_1/c(C^5_{2h}$; No. 14) with unit cell parameters at 173 K of $a = 17.036(3)$ Å, $b = 21.538(4)$ Å, $c = 14.441(2)$ Å, $\beta = 91.814(12)°$, $V = 5296.1(15)$ Å^3 and $D_{calcd} = 1.34$ g cm^{-3} for $Z = 8$. Least squares refinement of the model based on 5480 reflections ($|F_o| > 3.0\sigma(|F_o|)$) converged to a final $R_F = 5.0\%$. In the two independent molecules in the unit cell, the Me_3CNH_2 groups are attached to the bent metallocenes with 2.804(10) Å and 2.737(7) Å Sm–N distances and 112.4(8)° and 112.2(5)° Sm–N–C angles. The average Sm–C(C_5Me_5) distance is 2.816(16) Å and the (ring centroid)–Sm–(ring centroid) angles are 142.1° and 140.4°. $(C_5Me_5)_2Sm(THF)_2$ reacts with 2 equiv. of *N*-methylimidazole (N-MeIm) in THF to form THF soluble $(C_5Me_5)_2Sm(N\text{-}MeIm)_2$ (**2**) in quantitative yield. Compound **2** crystallizes from THF in the monoclinic space group $P2_1/c(C^5_{2h}$; No. 14) with unit cell parameters at 163 K of $a = 16.059(7)$ Å, $b = 10.291(4)$ Å, $c = 17.635(5)$ Å, $\beta = 101.00(3)°$, $V = 2861(2)$ Å^3 and $D_{calcd} = 1.36$ g cm^{-3} for $Z = 4$. Least squares refinement of the model based on 2824 reflections ($|F_o| > 4.0\sigma(|F_o|)$) converged to a final $R_F = 5.9\%$. The N-MeIm ligands are attached to the bent metallocene with Sm–N distances of 2.618(10) Å and 2.673(10) Å. The N–Sm–N angle is 84.2(3)° and the centroid–Sm–centroid angle is 138.0°. The average Sm–C(C_5Me_5) distance is 2.853(10) Å.

Keywords: Samarium; Rare earth metals; Metallocenes; Amine; Imidazole; Lanthanide

1. Introduction

As part of a continuing effort to probe the limits of reactivity of Sm^{II} in soluble organometallic complexes [1–5] and to develop new complexes of Sm^{II} with varying solubilities [6,7], we have examined the reaction of the Sm^{II} metallocenes $(C_5Me_5)_2Sm(THF)_x$ ($x = 0$–2) [8–10] with tert-butylamine, Me_3CNH_2, and N-methylimidazole, $\mathrm{Me\overline{NCH{=}CHN{=}C}H}$ (N-MeIm). We sought to determine if $(C_5Me_5)_2Sm(\text{N-donor})_x$ complexes would result by displacement of THF ligands from $(C_5Me_5)_2Sm(THF)_2$ [11] or by adduct formation from $(C_5Me_5)_2Sm$, or if a $Sm^{(III)}$ complex such as $(C_5Me_5)_2Sm(NR_2)$ would result either by reductive deprotonation [12] or reductive cleavage of C–N bonds [13].

We report here that tert-butylamine does not displace THF from $(C_5Me_5)_2Sm(THF)_x$ ($x = 1, 2$) [9,10], but it reacts with unsolvated $(C_5Me_5)_2Sm$ [8] to form an isolable divalent adduct of the $Sm^{(II)}$ metallocene. In contrast, N-MeIm displaces THF from $(C_5Me_5)_2Sm(THF)_2$ in THF to form a bis(N-MeIm) adduct analogous to $(C_5Me_5)_2Sm(THF)_2$.

2. Experimental section

The chemistry described below was performed under nitrogen and/or argon with rigorous exclusion of air and water by using Schlenk, vacuum line, and glovebox (Vacuum/Atmospheres HE-553 Dri-Lab) techniques. Physical measurements were obtained and

---

* Corresponding author.

0022-328X/94/$07.00
SSDI 0022-328X(94)24687-E

solvents were freshly distilled as previously described [14]. The complexes $(C_5Me_5)_2Sm(THF)_x$ ($x = 0$ [8], 1 [10], 2 [15]) were prepared according to the literature. Me_3CNH_2 (Aldrich) was vacuum transferred from molecular sieves.

2.1. $(C_5Me_5)_2Sm(NH_2CMe_3)$ (1)

Excess Me_3CNH_2 (0.5 ml) was added to dark green $(C_5Me_5)_2Sm$ (100 mg, 0.24 mmol) dissolved in 5 ml of toluene and caused an immediate color change to brownish-purple. The solvent was removed immediately to give **1** as a green powder. Subsequent crystallization from hexanes at −35°C gives **1** as green crystals (94 mg, 80%). ^1H NMR (C_6D_6, 300 MHz, 25°C, 0.062 M): δ 2.77 (br, $\nu_{1/2} = 16$ Hz, 30H, C_5Me_5), 2.6 (br, $\nu_{1/2} = 150$ Hz, 9H, CMe_3). ^{13}C NMR (C_6D_6, 300 MHz, 25°C): δ 97.0 (C_5Me_5), 40 (br, H_2NCMe_3), −91.0 (C_5Me_5). IR (Nujol): 3731 w, 3619 m, 3331 w, 2725 m, 2363 w, 1588 m, 1256 w, 1244 m, 1213 m, 1156 w, 1081 w, 1050 w, 1019 m, 988 w, 900 s, 800 m, 725 vs, 694 s, 669 w cm^{-1}. UV-VIS (hexane, λ_{max}, nm (ε)): 330 (1000), 290 (4700), 248 (6500). Magnetic susceptibility: $X_M^{294K} = 3.82 \times 10^{-3}$ cgs; $\mu_{eff} = 3.0\ \mu_B$. Anal. Calcd. for $C_{24}H_{41}NSm$: C, 58.35; H, 8.37; N, 2.84; Sm, 30.45. Found: C, 58.11; H, 8.18; N, 2.69; Sm, 30.70.

2.2. X-ray data collection, structure determination, and refinement for $(C_5Me_5)_2Sm(NH_2Me_3) \cdot (C_6H_6)_{0.5}$

Under nitrogen, a green crystal of approximate dimensions 0.13 × 0.27 × 0.33 mm was immersed in Paratone-D oil. The oil-coated crystal was then manipulated in air onto a glass fiber and transferred to the nitrogen stream of a Siemens P3 automated four-circle diffractometer which is equipped with a modified LT-2 low-temperature system. Determination of Laue symmetry, crystal class, unit cell parameters, and the crystal's orientation matrix were carried out by previously described methods similar to those of Churchill [16]. Intensity data were collected as described in Table 1.

All 7481 data were corrected for absorption and for Lorentz and polarization effects, and placed on an approximately absolute scale. The diffraction symmetry was $2/m$ with systematic absences $0k0$ for $k = 2n + 1$ and $h0l$ for $l = 2n + 1$. The centrosymmetric monoclinic space group $P2_1/n$, a non-standard setting of $P2_1/c$(C_{2h}^5; No. 14), is therefore uniquely defined.

All crystallographic calculations were carried out using either our locally modified version of the UCLA Crystallographic Computing Package [15] or the SHELXTL PLUS program set [16]. The analytical scattering factors for neutral atoms were used throughout the analysis [17a], both the real ($\Delta f'$) and imaginary ($i\Delta f''$) components of anomalous dispersion [17b] were included. The quantity minimized during least-squares analysis was $\Sigma w(|F_o| - |F_c|)^2$ where $w^{-1} = \sigma^2(|F_o|) + 0.0005(|F_o|)^2$.

The structure was solved by direct methods and refined by full-matrix least-squares techniques. There are two independent molecules in the asymmetric unit cell. There is also one-half molecule of benzene solvent present per formula unit. Hydrogen atoms were included using a riding model with d(C–H) = 0.96 Å and $U_{iso} = 0.08$ Å^2. The amine ligand in molecule 1 has higher thermal motion than expected and a more satisfactory refinement was obtained refining N(1) and C(21) isotropically. In molecule 2, similarly high thermal motion was not observed for the analogous atoms, N(2) and C(45). A final difference-Fourier synthesis yielded ρ(max) = 2.58 e Å^{-3} at a distance of 1.18 Å from N(1). Final fractional coordinates are given in Table 2.

Table 1
Experimental X-ray data for $(C_5Me_5)_2Sm(NH_2CMe_3) \cdot (C_6H_6)_{0.5}$ and $(C_5Me_5)_2Sm(N\text{-}MeIm)_2$ (2)

	$1 \cdot (C_6H_6)_{0.5}$	2
Formula	$C_{24}H_{41}NSm \cdot 1/2(C_6H_6)$	$C_{28}H_{42}N_4Sm$
FW	533.0	585.0
Temperature (K)	173	163
Crystal system	Monoclinic	Monoclinic
Space group	$P2_1/c$ (C_{2h}^5; No. 14)	$P2_1/c$ (C_{2h}^5; No. 14)
a (Å)	17.036(3)	16.059(7)
b (Å)	21.538(4)	10.291(4)
c (Å)	14.441(2)	17.635(5)
β (°)	91.814(12)	101.00(3)
V (Å^3)	5296.1(15)	2861(2)
Z	8	4
D_{calc} (mg m^{-3})	1.34	1.36
Diffractometer	Siemens P3 (R3m/v System)	Siemens P3 (R3m/v System)
Radiation	Mo Kα (λ = 0.710730 Å)	Mo Kα (λ = 0.710730 Å)
Monochromator	Highly oriented graphite	Highly oriented graphite
Data collected	$+h, +k, \pm l$	$+h, +k, \pm l$
Scan type	θ–2θ	θ–2θ
Scan width	1.20° plus Kα separation	1.20° plus Kα separation
Scan speed (in ω)	3.0° min^{-1}	3.0° min^{-1}
2θ range (°)	4.0–45.0	4.0–45.0
μ (Mo Kα) (mm^{-1})	2.24	2.08
Absorption correction	Semi-empirical (Ψ-scan method)	Semi-empirical (Ψ-scan method)
Reflections collected	7481	4238
Unique reflections with ($\lvert F_o \rvert > 0$)	6310	3447
Reflections with ($\lvert F_o \rvert > X\sigma(\lvert F_o \rvert)$)	5480 $X = 3.0$	2824 $X = 4.0$
No. of variables	513	298
R_F (%)	5.0	5.9
R_{wF} (%)	5.5	6.6
Goodness of fit	1.51	1.88

2.3. $(C_5Me_5)_2Sm(N\text{-}MeIm)_2$ (2)

N-MeIm (0.03 ml, 0.36 mmol) was added to $(C_5Me_5)_2Sm(THF)_2$ (100 mg, 0.18 mmol) dissolved in 5 ml of THF. The solvent was removed immediately. The residue was washed with toluene to give **2** as a dark purple powder (100 mg, 95%). ^1H NMR (C_4D_8O (0.046 M), 500 MHz, 25°C): δ 16.78 (v br, 2H, CH), 14.04 (v br, 2H, CH), 7.58 (s, 2H, CH), 5.92 (s, 6H, CH_3), 2.75 (s, 30H, C_5Me_5). ^{13}C NMR (C_4D_8O, 300 MHz, 25°C): δ 113.6 (CH), 98.9 ($C_5\mathit{Me}_5$), 30.4 (CH_3), −66.3 (C_5Me_5). IR (Nujol): 3670 m, 1590 m, 1525 s, 1521 s, 1517 s, 1416 s, 1285 s, 1230 s, 1110 s, 1083 s, 1024 m, 923 s, 825 m, 811 s, 765 m, 734 s, 662 s, 618 m cm^{-1}. UV-VIS (THF, λ_{max}, nm (ε)): 232 (21000), 350 (sh, 2000). Magnetic susceptibility: $X_M^{294K} = 3.99 \times 10^{-3}$ cgs; $\mu_{eff} = 3.1\ \mu_B$. Anal. Calcd. for $C_{28}H_{42}N_4Sm$: C, 57.48; H, 7.24; N, 9.58; Sm, 25.71. Found: C, 57.22; H, 7.09; N, 9.40; Sm, 25.60.

2.4. X-ray data collection, structure determination, and refinement for $(C_5Me_5)_2Sm(N\text{-}MeIm)_2$ (2)

Under nitrogen, a dark purple crystal of approximate dimensions 0.13 × 0.33 × 0.36 mm was handled as described above for **1** (see Table 1). The diffraction symmetry was $2/m$ with systematic absences $0k0$ for $k = 2n + 1$ and $h0l$ for $l = 2n + 1$. The centrosymmetric monoclinic space group $P2_1/c$ (C_{2h}^5; No.14) is therefore uniquely defined. All crystallographic calculations were carried out as described above for **1**. The quantity minimized during least-squares analysis was $\Sigma(|F_o| - |F_c|)^2$ where $w^{-1} = \sigma^2(|F_o|) + 0.0005(|F_o|)^2$.

The structure was solved by direct methods (SHELXTL PLUS) and refined by full-matrix least-squares techniques. Hydrogen atoms were included as described above. A final difference-Fourier synthesis yielded

Table 2
Final fractional coordinates for $(C_5Me_5)_2Sm(NH_2CMe_3) \cdot (C_6H_6)_{0.5}$

	x	*y*	*z*		*x*	*y*	*z*
Sm(1)	58507(3)	13507(2)	22422(3)	C(33)	101398(64)	69093(43)	13084(69)
C(1)	51643(57)	24588(39)	16179(59)	C(34)	84919(68)	69586(43)	22271(63)
C(2)	46667(52)	20120(40)	12439(59)	C(35)	103605(55)	96223(37)	22327(59)
C(3)	50802(49)	16953(39)	5495(54)	C(36)	107653(52)	92784(38)	15780(56)
C(4)	58308(53)	19600(39)	5085(58)	C(37)	111456(50)	87734(36)	20279(54)
C(5)	58882(54)	24312(37)	11907(59)	C(38)	109725(50)	88173(41)	29743(58)
C(6)	49710(67)	29381(43)	23716(66)	C(39)	105093(52)	93355(41)	31025(55)
C(7)	38165(55)	19321(51)	14427(69)	C(40)	99146(73)	102167(46)	20579(78)
C(8)	47467(65)	12028(45)	−730(67)	C(41)	108391(64)	94519(43)	5650(60)
C(9)	64468(59)	18022(48)	−2057(61)	C(42)	117275(54)	83378(45)	16157(62)
C(10)	66107(62)	28426(45)	13679(72)	C(43)	113230(59)	84033(48)	37317(65)
C(11)	67374(54)	5138(43)	33558(60)	C(44)	102948(65)	96184(49)	40443(65)
C(12)	65449(53)	1761(41)	25082(65)	N(2)	90133(43)	83469(34)	38489(47)
C(13)	69808(56)	4552(41)	18043(59)	C(45)	82685(55)	86901(44)	39791(62)
C(14)	74239(51)	9525(38)	21935(63)	C(46)	81921(56)	91811(43)	32365(64)
C(15)	72719(52)	9852(42)	31378(61)	C(47)	82580(57)	89723(52)	49243(59)
C(16)	65086(70)	3295(50)	43222(67)	C(48)	76165(58)	82238(50)	38827(72)
C(17)	60374(59)	−3860(43)	24305(73)	C(49)	36689(75)	54677(53)	74588(99)
C(18)	70037(69)	2202(45)	8303(63)	C(50)	30696(104)	54524(54)	80788(84)
C(19)	80109(57)	13471(47)	17106(73)	C(51)	24299(76)	50688(63)	78735(100)
C(20)	76443(69)	14353(53)	38215(82)	C(52)	24322(77)	47088(55)	71042(96)
N(1)	53776(64)	16702(49)	40220(69)	C(53)	30007(91)	47449(54)	65376(81)
C(21)	46466(87)	14182(61)	42257(98)	C(54)	36167(73)	51002(56)	66753(81)
C(22)	44307(63)	9131(46)	35795(67)				
C(23)	46445(97)	11902(73)	52104(91)				
C(24)	40404(83)	18728(65)	42095(100)				
Sm(2)	95525(3)	84790(2)	20946(3)				
C(25)	83149(51)	78850(38)	10634(56)				
C(26)	87855(53)	81477(37)	3956(54)				
C(27)	94980(52)	78397(38)	3871(56)				
C(28)	94900(55)	73728(38)	10713(58)				
C(29)	87577(53)	74007(37)	14968(56)				
C(30)	74659(57)	80357(50)	12138(63)				
C(31)	85213(62)	86789(41)	−2369(62)				
C(32)	101507(58)	79584(44)	−3053(58)				

Table 3
Final fractional coordinates for $(C_5Me_5)_2Sm(N\text{-}MeIm)_2$ (2)

	x	y	z
Sm(1)	24987(4)	8178(6)	22044(3)
N(1)	35600(60)	14512(103)	13087(48)
N(2)	45921(61)	15948(98)	6452(51)
N(3)	15162(63)	26526(110)	14170(52)
N(4)	11456(74)	46240(95)	10495(53)
C(1)	25783(65)	−19548(111)	20486(62)
C(2)	17970(70)	−17051(111)	23096(59)
C(3)	12143(69)	−10668(117)	17019(65)
C(4)	16512(75)	−9226(125)	10614(59)
C(5)	24750(74)	−14760(118)	12826(62)
C(6)	33391(73)	−25979(133)	24568(72)
C(7)	15574(89)	−21876(133)	30478(70)
C(8)	3109(72)	−7533(140)	17116(75)
C(9)	12467(82)	−4214(130)	2804(63)
C(10)	31197(85)	−16442(133)	7828(69)
C(11)	24411(69)	17292(110)	37208(54)
C(12)	26847(68)	28446(102)	33358(56)
C(13)	35370(70)	26052(125)	32123(56)
C(14)	37870(69)	13501(114)	35095(59)
C(15)	31236(70)	8183(119)	38268(55)
C(16)	15970(77)	15953(132)	39699(65)
C(17)	22019(81)	40964(126)	31904(70)
C(18)	40828(86)	35700(132)	28720(72)
C(19)	46444(74)	7221(136)	35405(68)
C(20)	31833(84)	−3951(121)	42868(70)
C(21)	43836(79)	13347(122)	13448(65)
C(22)	38472(86)	18881(129)	1607(65)
C(23)	32395(84)	18003(131)	5582(66)
C(24)	54260(82)	15424(158)	4547(79)
C(25)	17774(88)	37593(140)	12294(70)
C(26)	4331(90)	39976(146)	11277(86)
C(27)	6747(87)	27843(164)	13515(80)
C(28)	12373(108)	59379(151)	8311(83)

$\rho(\max) = 1.58$ e Å^{-3}. Final fractional coordinates are given in Table 3.

3. Results

3.1. $(C_5Me_5)_2Sm(NH_2CMe_3)$ (1)

The purple complex $(C_5Me_5)_2Sm(THF)_2$ shows no color change and no evidence of reaction when treated with Me_3CNH_2 in THF. When the same reaction is done in toluene, the dark green mono-solvate, $(C_5Me_5)_2Sm(THF)$, is recovered. However, addition of Me_3CNH_2 to dark green $(C_5Me_5)_2Sm$ in toluene causes an immediate color change to brownish-purple. Removal of solvent leaves $(C_5Me_5)_2Sm(NH_2CMe_3)$ (1) as a green solid in quantitative yield. Complex 1 was characterized by elemental analysis and NMR and IR spectroscopy and was identified by X-ray crystallography (Fig. 1). Samples of $(C_5Me_5)_2Sm(THF)_x$ ($x = 0$–2) dissolved in neat tert-butylamine generate a purple solution which gives a purple solid upon removal of solvent. This material, which exhibits different NMR signals (C_5Me_5 resonance at δ 2.01 ppm) from 1, may be the disolvate $(C_5Me_5)_2Sm(NH_2CMe_3)_2$, but definitive data on it were not obtained. In THF, both this material and 1 revert directly back to $(C_5Me_5)_2Sm(THF)_2$.

The ^1H NMR spectrum of 1 contains broad peaks and is concentration dependent as is typical for the $(C_5Me_5)_2Sm(THF)_x$ complexes [8,9]. The ^{13}C NMR spectrum of 1 has the distinctive shifts characteristic of C_5Me_5 $Sm^{(II)}$ compounds [12]; the C_5Me_5 ring carbons resonate at −91.0 ppm and the C_5Me_5 methyl carbons resonate at 97.0 ppm. The color of 1 and its intensity are also characteristic of $Sm^{(II)}$ rather than $Sm^{(III)}$ [1,20]. Complex 1 is more soluble in alkane solvents (ca. 0.05 M in hexane) than its THF counterpart $(C_5Me_5)_2Sm(THF)$ (ca. 0.01 M), but both of these mono-solvates are less soluble than $(C_5Me_5)_2Sm$ in hexane (ca. 0.1 M).

Compound 1 crystallizes from benzene with two independent molecules in the unit cell. Hence, there are two sets of values in Table 4. The structural parameters on 1 are similar to those for the monosolvates $(C_5Me_5)_2Sm(THF)$ (3) [10] and $(C_5Me_5)_2Sm$(tetrahydropyran) (4) [21]. The 2.781(8)–2.846(8) Å range of Sm–C(C_5Me_5) distances is within the 2.770(9)–2.858(6) Å range found for 3 and 4 and the 2.82(2) Å averages for each molecule of compound 1 are identical to the averages for 3 and 4. The 140.4° and 142.1° (ring centroid)–Sm–(ring centroid) angles are also similar to the 138.5 and 140.0° values for 3 and 4, respectively. All of these values are very typical of Sm^{II} bent metallocenes [22].

The nitrogen donor atom of the tert-butylamine ligand is not located symmetrically in this complex. The disparate 111.8 and 101.9° N–Sm–(ring centroid) angles (115.7 and 101.5 in molecule 2 in the unit cell)

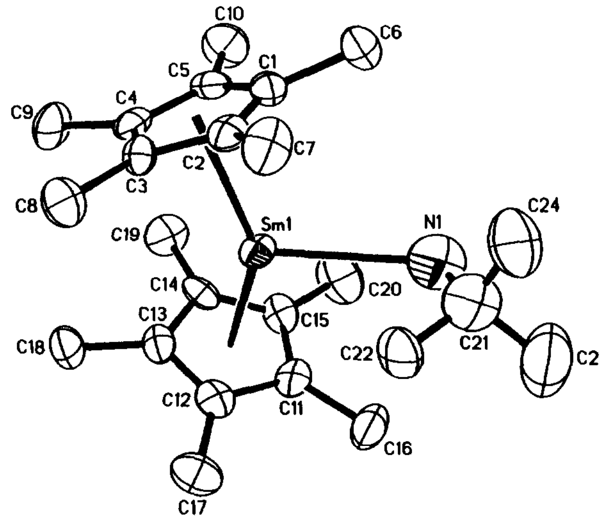

Fig. 1. Thermal ellipsoid plot of $(C_5Me_5)_2Sm(NH_2CMe_3)$ (1) drawn at the 50% probability level.

Table 4
Selected bond lengths (Å) and angles (°) for $(C_5Me_5)_2Sm(NH_2CMe_3)$ (1)

Sm(1)–C(1)	2.795(9)	Sm(2)–C(25)	2.846(8)
Sm(1)–C(2)	2.827(9)	Sm(2)–C(26)	2.834(8)
Sm(1)–C(3)	2.837(8)	Sm(2)–C(27)	2.823(8)
Sm(1)–C(4)	2.826(8)	Sm(2)–C(28)	2.804(8)
Sm(1)–C(5)	2.781(8)	Sm(2)–C(29)	2.810(8)
Sm(1)–C(11)	2.822(9)	Sm(2)–C(35)	2.825(8)
Sm(1)–C(12)	2.814(9)	Sm(2)–C(36)	2.808(9)
Sm(1)–C(13)	2.811(9)	Sm(2)–C(37)	2.792(8)
Sm(1)–C(14)	2.817(9)	Sm(2)–C(38)	2.793(8)
Sm(1)–C(15)	2.821(9)	Sm(2)–C(39)	2.833(9)
Sm(1)–N(1)	2.804(10)	Sm(2)–N(2)	2.737(7)
N(1)–C(21)	1.398(18)	N(2)–C(45)	1.486(12)
C(21)–C(22)	1.472(17)	C(45)–C(46)	1.509(13)
C(21)–C(23)	1.505(19)	C(45)–C(47)	1.495(13)
C(21)–C(24)	1.423(20)	C(45)–C(48)	1.501(14)
N(1)–Sm(1)–Cnt(1)	111.8	N(2)–Sm(2)–Cnt(3)	115.7
N(1)–Sm(1)–Cnt(2)	101.9	N(2)–Sm(2)–Cnt(4)	101.5
Cnt(1)–Sm(1)–Cnt(2)	142.1	Cnt(3)–Sm(2)–Cnt(4)	140.4
Sm(1)–N(1)–C(21)	112.4(8)	Sm(2)–N(2)–C(45)	112.2(5)
N(1)–C(21)–C(22)	111.1(11)	N(2)–C(45)–C(46)	108.3(7)
N(1)–C(21)–C(23)	110.8(12)	N(2)–C(45)–C(47)	110.7(7)
N(1)–C(21)–C(24)	112.3(11)	N(2)–C(45)–C(48)	106.7(8)

show the asymmetry of the nitrogen between the rings. The nitrogen atom location also has a side to side asymmetry as shown in Fig. 2. A symmetrically located nitrogen donor atom would be coplanar with the samarium and the two C_5Me_5 ring centroids. In 1, the nitrogen lies 1.26 Å out of this plane. Alternatively, the asymmetry can be described by the fact that samarium lies 0.30 Å out of the plane defined by the two C_5Me_5 centroids and nitrogen. Both 3 and 4 show lateral asymmetry for the oxygen donor atom with oxygen lying 0.42 Å and 0.34 Å, respectively, out of the centroid–Sm–centroid plane, but the oxygen atoms in these complexes are located midway between the two planes.

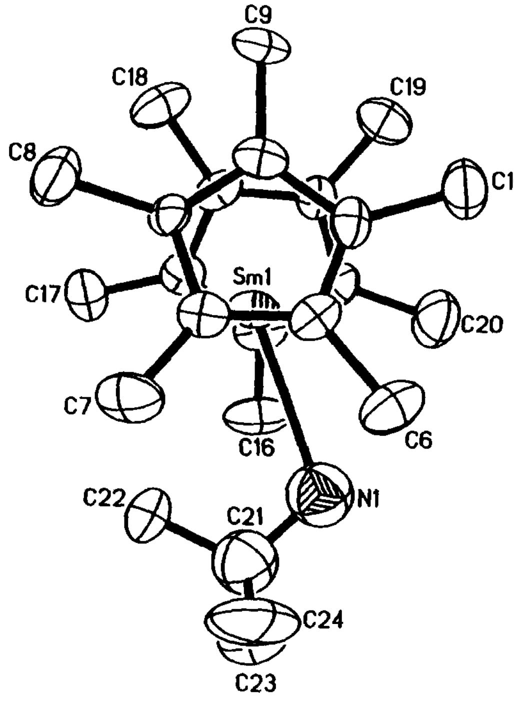

Fig. 2. Top view of the thermal ellipsoid plot of $(C_5Me_5)_2Sm(NH_2CMe_3)$ (1).

Although the structures of 3 and 4 show no special need for this asymmetry, in 1, the position of the methyl group of C(22) could be responsible via agostic hydrogen interaction. The nonbonding distance from this methyl carbon to samarium is 3.29 Å and the analogous value is 3.26 Å in molecule 2 in the unit cell (involving C(46)). These distances are very long compared to the $Sm–C(C_5Me_5)$ distances, but they are comparable to the closest intermolecular Sm–C(Me) distance in divalent $(C_5Me_5)_2Sm$ [8] which is 3.22(1) Å. The 112.4(8) and 112.2(5) Sm–N–C(tert-butyl) angles may be somewhat smaller than expected, but the N–C–C angle involving the nearest methyl group is not statistically distinguishable from the other analogous angles.

The Sm–N distances in 1 are 2.737(7) and 2.804(10) Å. These are considerably longer than the 2.569(3) and 2.630(6) Å Sm–O distances in 3 and 4, respectively, as would be expected. For example, in $(C_5Me_5)_2Yb(THF)(NH_3)$ [23] the $Yb–N(NH_3)$ distance is 2.55(3) Å and the Yb–O(THF) distance is 2.46(3) Å. Similarly, in the complexes, $(C_5Me_5)_2Yb(SPh)(NH_3)$ [24] and $(C_5Me_5)_2Yb(TePh)(NH_3)$ [25], the crystallographically independent Yb–N distances are 2.50(1), 2.432(8), and 2.423(8) Å, whereas in other eight coordinate $(C_5Me_5)_2YbZ(THF)$ complexes, the Yb–O(THF) distances range from 2.330(3) Å to 2.37 Å [22].

3.2. $(C_5Me_5)_2Sm(N\text{-}MeIm)_2$ (2)

In contrast to tert-butylamine, N-methylimidazole readily displaces the THF ligands in $(C_5Me_5)_2Sm(THF)_2$ in THF solution to form a bis(N-MeIm) adduct (2). The purple 2, like 1, has ^1H and ^{13}C NMR spectra characteristic of $Sm^{(II)}$. Elemental analysis indicated that a bis(N-MeIm) adduct had formed and this was confirmed by X-ray crystallography as shown in Fig. 3. In contrast to 1, 2 is less soluble than its THF counterpart; it is insoluble in toluene, but readily dissolves in THF with a solubility of 0.15 M compared to 0.35 M for $(C_5Me_5)_2Sm(THF)_2$. The fact that the N-MeIm-solvated 2 is recovered from THF is consistent with the strong binding exhibited by N-MeIm to a variety of metals [26,27].

The X-ray crystal structure of 2 allows some direct comparisons between N-methylimidazole and THF as solvating ligands for lanthanide complexes. Selected bond distances and angles for 2 are given in Table 5. The overall structures of 2 and $(C_5Me_5)_2Sm(THF)_2$ (5)

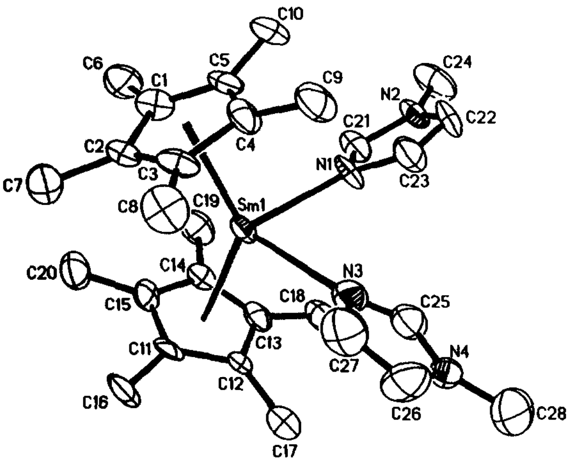

Fig. 3. Thermal ellipsoid plot of $(C_5Me_5)_2Sm(N\text{-}MeIm)_2$ (2) drawn at the 50% probability level.

are similar with 138.0 and 136.5° centroid–Sm–centroid angles and 84.2(3) and 82.5(3)° N(O)–Sm–N(O) angles, respectively. The centroid–Sm–donor atom angles are also similar. The 2.85(1) Å Sm–C(C_5Me_5) average distance in **2** is not different within the error limits from the 2.86(2) and 2.87(2) values in **5**. The similarity of these parameters is not unexpected. However, it is surprising that the Sm–donor atom distances are also quite similar: 2.618(10) and 2.673(10) in **2** and 2.614(7) and 2.652(8) Å in **5**. Hence, in all of these metrical aspects, N-methylimidazole appears to sterically mimic THF in this $Sm^{(II)}$ system. Fig. 4 shows a superposition of **2** and **5** which reveals the extent of the similarity. The analogous side view shows that the two $(C_5Me_5)_2Sm$ units are coincident except for the arrangement of the methyl groups around the C_5Me_5 rings. Fig. 4 shows the coincidence of the metal and the oxygen and nitrogen donor atoms: the weighted root mean square deviation of Sm and the two N donor atoms in **2** and Sm and the two O donor atoms in **5** is 0.03 Å. The main difference in the two structures is the orientation of the N-MeIm ligands versus the THF ligands as shown.

Table 5
Selected bond lengths (Å) and angles (°) for $(C_5Me_5)_2Sm(N\text{-}MeIm)_2$ (2)

Sm(1)–C(1)	2.872(12)
Sm(1)–C(2)	2.850(12)
Sm(1)–C(3)	2.847(11)
Sm(1)–C(4)	2.842(11)
Sm(1)–C(5)	2.862(12)
Sm(1)–C(11)	2.852(10)
Sm(1)–C(12)	2.862(10)
Sm(1)–C(13)	2.862(11)
Sm(1)–C(14)	2.839(10)
Sm(1)–C(15)	2.846(9)
Sm(1)–N(1)	2.618(10)
Sm(1)–N(3)	2.673(10)
N(1)–Sm(1)–N(3)	84.2(3)
N(1)–Sm(1)–Cnt(1)	103.1
N(1)–Sm(1)–Cnt(2)	104.9
N(3)–Sm(1)–Cnt(1)	108.4
N(3)–Sm(1)–Cnt(2)	104.9
Cnt(1)–Sm(1)–Cnt(2)	138.0

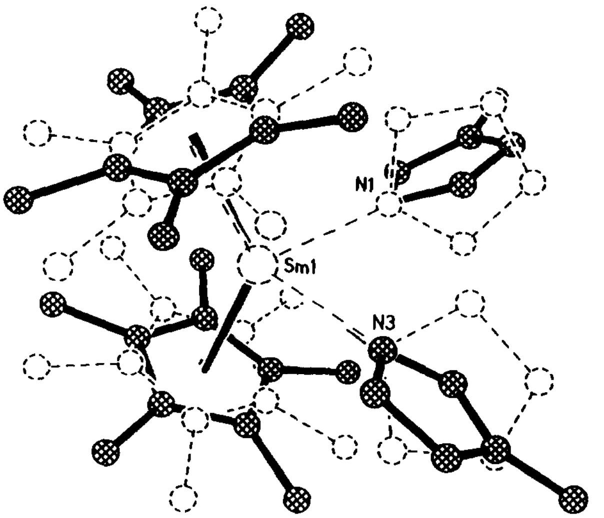

Fig. 4. Ball and stick diagram of 2 superimposed on the ball and stick diagram of $(C_5Me_5)_2Sm(THF)_2$ (5) (dotted lines).

The similarity of the Sm–N(N–MeIm) distances to the Sm–O(THF) distances is surprising in light of the data discussed above for **1** which show that Ln–O distances are typically shorter than Ln–N distances. The 2.646(19) Å average Sm–N distance in **2** also appears to be short compared to the 2.77(2) Å average in **1**, despite the fact that **2** has a higher formal coordination number which should lead to a larger value. Comparison can also be made with the pyridine complex, $(C_5Me_5)_2Yb(NC_5H_5)_2$ [28], which has Yb–N distances of 2.586(7) and 2.544(6) Å. Considering that eight coordinate $Yb^{(II)}$ is 0.13 Å smaller than eight coordinate $Sm^{(II)}$ according to Shannon [29], the comparable Sm–N distances would be expected to be 2.67–2.72 Å. All of these comparative data are consistent with a strong attachment of the N-MeIm ligand to samarium.

4. Discussion

The formation of nitrogen base adducts with divalent lanthanide metallocenes has previously been observed between $(C_5Me_5)_2Yb$ and pyridine [28] and NH_3 [23]. With the more strongly reducing $Sm^{(II)}$, other reactivity patterns are possible including metallation [12,30] and C–N bond cleavage [13,31]. Using tert-butylamine and N-methylimidazole as the nitrogen bases, these alternative reaction pathways are not observed and simple adduct formation occurs. Tert-butylamine is not a strong enough donor to displace THF from $(C_5Me_5)_2Sm(THF)_{1,2}$ in solution, but the more powerful N-methylimidazole readily accomplishes this reaction to make a nitrogen analog of $(C_5Me_5)_2Sm(THF)_2$. N-Methylimidazole has previously been shown to be an excellent donor ligand for transition metal [26] and lanthanide complexes [27].

Derivatizing the $(C_5Me_5)_2Sm(THF)_x$ systems with these nitrogen donors has a significant effect on the solubilities. Hence, by forming the tert-butylamine monosolvate, a $Sm^{(II)}$ complex more soluble in alkanes than $(C_5Me_5)_2Sm(THF)$ is obtained and by using N-MeIm, a complex less soluble than $(C_5Me_5)_2Sm(THF)_2$ in arenes results. These fully characterized complexes can now be used for reaction chemistry which may have specific solubility needs not met by the $(C_5Me_5)_2Sm(THF)_x$ reagents. Another way in which these results can be used in other systems is to use N-MeIm to remove toluene soluble $(C_5Me_5)_2Sm(THF)_x$ complexes from a mixture which has some other desirable soluble component which does not react with N-MeIm. Simple addition of N-MeIm may precipitate $(C_5Me_5)_2Sm(N\text{-}MeIm)_2$ and eliminate the mixture.

Although it is not established that there is any direct connection between the enhanced solubility of **1** and the use of a monodentate donor ligand which has a methyl group which can fill in an open coordination position, it is possible that this approach may be a useful one in controlling solubility. To the extent that the special properties found for the $Sm^{(II)}$ metallocenes arise from the protective environment provided by the ligands [32], variations of the solvated species available should provide additional opportunities to precisely control reactivity.

5. Conclusion

The solubility of the $(C_5Me_5)_2Sm$ unit can be controlled by varying the base adducts attached to the metal. Attachment of tert-butylamine gives a soluble monosolvated species which contains a methyl group in an otherwise open coordination position. Addition of N-methylimidazole forms a disolvated complex which is less soluble but nearly isostructural with $(C_5Me_5)_2Sm(THF)_2$.

Acknowledgment

We thank the National Science Foundation for support for this research and the Stiftung Stipendien-Fonds des Verbandes der Chemischen Industrie, Germany, for the award of a Liebig-fellowship (to G.W.R).

References

[1] W.J. Evans, *Polyhedron, 6* (1987) 803.
[2] W.J. Evans, T.A. Ulibarri and J.W. Ziller, *J. Am. Chem. Soc., 110* (1988) 6877.
[3] W.J. Evans and D.K. Drummond, *J. Am. Chem. Soc., 110* (1988) 2772.
[4] W.J. Evans, T.A. Ulibarri and J.W. Ziller, *J. Am. Chem. Soc., 112* (1990) 219.
[5] W.J. Evans, S.L. Gonzales and J.W. Ziller, *J. Am. Chem. Soc., 114* (1991) 9880.
[6] W.J. Evans, T.S. Gummersheimer, T.J. Boyle and J.W. Ziller, *Organometallics, 13* (1994) 1281.
[7] W.J. Evans, G.W. Rabe and J.W. Ziller, *Organometallics, 13* (1994) 1641.
[8] W.J. Evans, L.A. Hughes and T.P. Hanusa, *Organometallics, 5* (1986) 1285.
[9] W.J. Evans, J.W. Grate, H.W. Choi, I. Bloom, W.E. Hunter and J.L. Atwood, *J. Am. Chem. Soc., 107* (1985) 941.
[10] W.J. Evans, G. Kociok-Köhn, S.E. Foster, J.W. Ziller and R.J. Doedens, *J. Organomet. Chem., 444* (1993) 61.
[11] W.J. Evans, T.A. Ulibarri, L.R. Chamberlain, J.W. Ziller and D. Alvarez, *Organometallics, 9* (1990) 2124.
[12] W.J. Evans and T.A. Ulibarri, *J. Am. Chem. Soc., 109* (1987) 4292.
[13] W.J. Evans, D.K. Drummond, H. Zhang and J.L. Atwood, *Organometallics, 7* (1988) 797.
[14] W.J. Evans, L.R. Chamberlain, T.A. Ulibarri and J.W. Ziller, *J. Am. Chem. Soc., 110* (1988) 6423.
[15] W.J. Evans and T.A. Ulibarri, *Inorg. Synth., 27* (1990) 155.
[16] M.R. Churchill, R.A. Lashewycz and F.J. Rotella, *Inorg. Chem., 16* (1977) 265.
[17] (a) *UCLA Crystallographic Computing Package*, University of California, Los Angeles, 1981; (b) C. Strouse, personal communication.
[18] G.M. Sheldrick, Siemens Analytical X-ray Instruments, Inc., Madison, WI 1990.
[19] *International Tables for X-Ray Crystallography* 1992, Vol. C, Kluwer, Dordrecht.
[20] G.H. Dieke, in H.M. Crosswhite and H. Crosswhite (eds.), *Spectra and Energy Levels of Rare Earth Ions in Crystals*, Wiley, New York, 1968.
[21] W.J. Evans and T.A. Ulibarri, *Polyhedron, 8* (1989) 1007.
[22] W.J. Evans and S.E. Foster, *J. Organomet. Chem., 433* (1992) 94.
[23] A.L. Wayda, J.L. Dye and R.D. Rogers, *Organometallics, 3* (1984) 1605.
[24] A. Zalkin, T.J. Henly and R.A. Andersen, *Acta Crystallogr.*, Sect. C, *43* (1987) 233.
[25] D.J. Berg, R.A. Andersen and A. Zalkin, *Organometallics, 7* (1988) 185.
[26] S. Dev, E. Ramli, T.B. Rauchfuss and C.L. Stern, *J. Am. Chem. Soc., 112*, (1990) 6385. S. Dev, E. Ramli, T.B. Rauchfuss and S.R. Wilson, *Inorg. Chem., 30* (1991) 2514. E. Ramli, T.B. Rauchfuss and C.L. Stern, *J. Am. Chem. Soc., 112* (1990) 4043. T.B. Rauchfuss, S. Dev and S.R. Wilson, *Inorg. Chem., 31* (1992) 154. M.E. Wozniak, A. Sen and A.L. Rheingold, *Chem Mater., 4* (1992) 753.
[27] W.J. Evans, G.W. Rabe and J.W. Ziller, *Inorg. Chem.*, 33 (1994) 3072.
[28] T.D. Tilley, R.A. Andersen, B. Spencer and A. Zalkin, *Inorg. Chem., 21* (1982) 2647.
[29] R.D. Shannon, *Acta Crystallogr.*, Sect. A, *32* (1976) 751.
[30] W.J. Evans, G. Kociok-Köhn, V.S. Leong and J.W. Ziller, *Inorg. Chem., 31* (1992) 3592.
[31] W.J. Evans, S.E. Foster and J.W. Ziller, unpublished.
[32] W.J. Evans, *J. Alloys Compd., 192* (1993) 205 and refs. therein.